Internal Force-Based Impedance Control for Cooperating Manipulators [1]

Robert G. Bonitz and T.C. Hsia
Systems, Control, Robotics Laboratory
Department of Electrical and Computer Engineering
University of California, Davis
Davis, CA 95616

February 1996

[1]This work supported in part by the NITTA Corporation of Japan.

Abstract

An internal force-based impedance control scheme for cooperating manipulators is introduced which controls the motion of the objects being manipulated and the internal force on the objects. The controller enforces a relationship between the velocity of each manipulator and the internal force on the manipulated objects. Each manipulator is directly given the properties of an impedance by the controller, thus, eliminating the gain limitation inherent in the structure of previously proposed schemes. The controller uses the forces sensed at the robot end effectors to compensate for the effects of the objects' dynamics and to compute the internal force using only kinematic relationships. Thus, knowledge of the objects' dynamics is not required. Stability of the system is proven using Lyapunov theory and simulation results are presented validating the proposed concepts. The effect of computational delays in digital control implementations is analyzed vis-a-vis stability and a lower bound derived on the size of the desired manipulator inertia relative to the actual manipulator endpoint inertia. The bound is independent of the sample time.

1 Introduction

Multiple robots performing tasks together in a cooperative manner can have a significant advantage over a single robot just as a human being using two arms has an advantage over one using one arm and multiple humans have an advantage over a single human. If the load is heavier than the carrying capacity of a single robot, multiple robots can distribute the load among them and move the object where the single robot would not be able to do so. In assembly tasks multiple robots can handle several objects at once increasing the speed of assembly and obviating the need for special fixturing. Assembly of objects in space is made easier where there is no fixed workbench on which to mount the single robot.

Various controllers for cooperating multiple robots have been proposed during recent years. They may be generally classified as position/force control [1, 2, 3, 4, 5, 6, 7, 8] or

impedance control [9, 10, 11, 12, 13, 14]. In position/force control the extra degrees of freedom of the multiple arm system are used to control internal force. The required joint torques are the sum of torques from the position and force control loops. Impedance control has generally been implemented by adding a force loop around a position controller. Sensed force is used to make corrections to the commanded trajectory via an admittance/compliance relationship. The modified trajectory is the input to the position controller.

Problems have been reported in tuning the Cartesian position control gains in the hybrid position/force control scheme [1] and the force loop was modified to become a compliance to reduce computational complexity. This effectively turned the scheme into an impedance control scheme.

In [14] both absolute and relative position of the object and absolute and internal force on the object are defined as in [1] and an impedance control scheme is implemented in object position space (absolute and relative). Gravity compensation for each arm is provided, but not for the object so object dynamics will contribute to tracking error. Another drawback is the difficulty of specifying the absolute and relative orientation of the object whose meaning is not clear. The problem is resolved by specifying the control in the desired task space, transforming to joint space via inverse kinematics, and then transforming again to object space. This has the drawback, however, of requiring the inverse kinematics. The scheme does not require force sensors which is simpler and cheaper to implement, but it is difficult to regulate the force to some desired level without them. Also, it should be noted that in [15] better results were obtained with force feedback when implementing impedance control on a single manipulator.

The object impedance control scheme in [12] enforces an impedance of the object rather than the manipulator endpoints. The experimental results are quite good, but the scheme does require knowledge of the object dynamics which may not always be known. Endpoint impedance control was also investigated, but as expected the tracking performance is not as good due to the effect of the object inertial forces.

Impedance control for cooperating manipulators should enforce a relationship between velocity and internal force. Otherwise, the object dynamics can contribute to tracking and steady-state position errors. Most of the previously proposed impedance controllers for cooperating manipulators do not adequately address this phenomenon. [13] does not consider the object dynamics at all and [10] includes only a gravity term. The virtual internal model scheme of [11] does include the object dynamics, but it is model based and requires knowledge of the object dynamics and so is limited to applications where the object properties are well known. Also, since it is implemented by feeding back the sensed force via an admittance function, the size of the admittance function must be less than the size of the reciprocal of the forward loop mapping to assure stability [16]. Thus, the gain of the admittance function is limited by the gain of the position controller.

The internal force-based impedance control scheme presented in this paper embodies two key concepts which are an improvement over previously proposed schemes:

1. Internal force is used in the impedance relationship by computing it from the sensed forces at the robot end effectors using only kinematic relationships. Thus, the dynamics of the manipulated objects do not contribute to tracking and steady-state position error and knowledge of the object dynamics is not required.

2. Each manipulator is directly given the property of an impedance by the controller. This eliminates the need to have both a position and force control loop and the impedance parameters (i.e., gains) are not limited by a given position controller.

In section 6 the effects of computational delays are analyzed vis-a-vis system stability and the choice of parameters in the proposed internal force-based impedance control law. It is shown that there exists a lower bound on the size of the desired inertia matrix which is independent of the sample time. This independence has implications even when simulating the continuous-time control system as there is always some inherent delay due to the integration time period.

2 System

Consider the system of n robots handling an object as shown in Figure 1. The object could consist of multiple objects in contact with each other during an assembly task. Each manipulator grasps the object rigidly and, thus, may exert both a force and a moment on the object. We define the following nomenclature with all vectors expressed in the Cartesian world frame:

x_i = Cartesian position and orientation of the ith robot end-effector frame

$p_i = [p_{ix}\ p_{iy}\ p_{iz}]^T$ = the vector from ith the end-effector frame to the object frame

f_i = force exerted by the ith robot end effector

m_i = moment exerted by the ith robot end effector

$\tilde{f}_i = [f_i\ \ m_i]$ = force/moment applied by the ith robot end effector

$\tilde{f} = [\tilde{f}_1^T\ ...\ \tilde{f}_n^T]^T$ = combined force vector

$\tilde{f}_M$ = motion-inducing force/moment applied by the manipulators

$\tilde{f}_I$ = internal force/moment applied by the manipulators

$\tilde{f}_o = [f_o^T\ m_o^T]^T$ = net force and moment at the object

J_{oi} = Jacobian from the object frame to the ith end-effector frame

$J_o = [J_{o1}^T(p_1)\ ...\ J_{on}^T(p_n)]^T$ = combined object Jacobian

τ_i = joint torque vector for the ith robot

q_i = the vector of joint variables for the ith robot

$D_i(q_i)$ = inertia matrix of the ith robot

$E_i(q_i, \dot{q}_i)$ = Coriolis, centripetal, and gravity vector for the ith robot

$J_i(q_i)$ = Jacobian of the ith robot

The dynamic equation for each manipulator is described by

$$\tau_i = D_i(q_i)\ddot{q}_i + E_i(q_i, \dot{q}_i) + J_i^T(q_i)\tilde{f}_i. \tag{1}$$

The function arguments are suppressed subsequently for convenience.

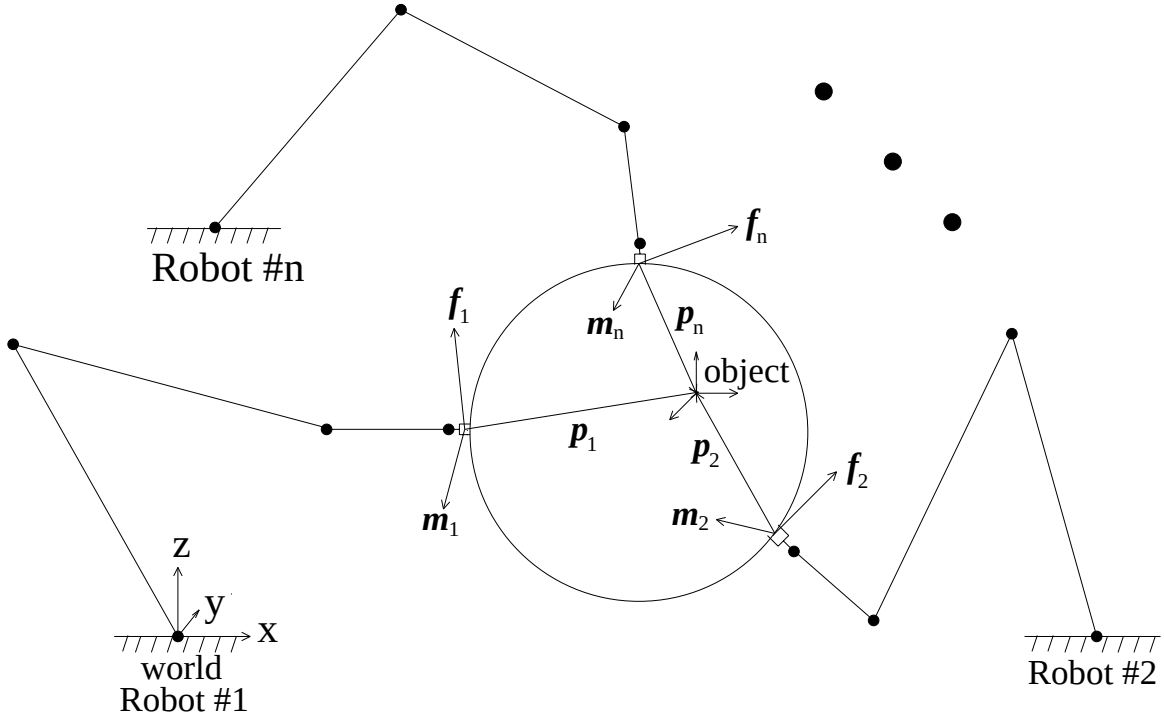

Figure 1: n-Manipulator System

3 Internal force

When multiple manipulators grasp an object, the force applied by the manipulators may be decomposed into motion-inducing and internal force. Internal force consists of compressive or tensile force and torsion. Our objective in this section is to decompose the applied force, $\tilde{f}$, into its motion-inducing, $\tilde{f}_M$, and internal, $\tilde{f}_I$, components with

$$\tilde{f} = \tilde{f}_M + \tilde{f}_I. \tag{2}$$

When the manipulators grasp the object rigidly, the net force at the object frame is related to the forces applied by the manipulators by

$$\tilde{f}_o = [J_{o1}^T \cdots J_{on}^T]\tilde{f} = J_o^T \tilde{f} \tag{3}$$

where

$$J_{oi}^T = \begin{bmatrix} I_3 & O_3 \\ -P_i & I_3 \end{bmatrix} \text{ and } P_i = p_i\times = \begin{bmatrix} \mathbf{0} & -p_{iz} & p_{iy} \\ p_{iz} & \mathbf{0} & -p_{ix} \\ -p_{iy} & p_{ix} & \mathbf{0} \end{bmatrix}. \tag{4}$$

The internal component produces no net force on the object and, thus, lies in the null space of J_o^T. Using this fact we get from (2) and (3) the following decomposition

$$\tilde{f}_M = J_o^{T\#} J_o^T \tilde{f} \text{ and } \tilde{f}_I = (I - J_o^{T\#} J_o^T)\tilde{f} \tag{5}$$

where $J_o^{T\#}$ is a generalized inverse of J_o^T. The generalized inverse, $J_o^{T\#}$, and, hence, (5) depends on the metrics chosen for the space of applied forces, $\tilde{\mathcal{F}}$, and the space of net forces on the object, $\tilde{\mathcal{F}}_o$, [17]. Equivalent solutions to (5) have been presented in [6, 18, 19] with

$$J_o^{T\#} = \frac{1}{n}\begin{bmatrix} I_3 & O_3 \\ P_1 & I_3 \\ \vdots & \vdots \\ I_3 & O_3 \\ P_n & I_3 \end{bmatrix} = \frac{1}{n}\begin{bmatrix} J_{o1}^{-T} \\ \vdots \\ J_{on}^{-T} \end{bmatrix}. \tag{6}$$

As pointed out in [18], the above solution results in zero internal loading anywhere in the object when $f_I = \mathbf{0}$. See [20] for a detailed discussion of internal force in cooperating manipulators including solutions to systems with non-rigid grasping. It should also be noted that the projection operator onto the internal-force subspace, $I - J_o^{T\#} J_o^T$, does not depend on the object Jacobian. To show this fact we perform the matrix multiplication

$$J_o^{T\#} J_o^T = \frac{1}{n}\begin{bmatrix} I_6 & J_{o1}^{-T} J_{o2}^T & \cdots & J_{o1}^{-T} J_{on}^T \\ J_{o2}^{-T} J_{o1}^T & I_6 & \cdots & J_{o2}^{-T} J_{on}^T \\ \vdots & \vdots & \ddots & \vdots \\ J_{on}^{-T} J_{o1}^T & J_{on}^{-T} J_{o2}^T & \cdots & I_6 \end{bmatrix} \tag{7}$$

where for $i, j = 1, 2, ...n$

$$J_{oi}^{-T} J_{oj}^T = \begin{bmatrix} I_3 & O_3 \\ P_i - P_j & I_3 \end{bmatrix} \tag{8}$$

Thus, $I - J_o^{T\#} J_o^T$ depends only on the vector from each end-effector frame to each other end-effector frame and not the object Jacobian. This matches our intuition as internal force should not be a function of where the object frame is located. It also permits us to choose any suitable frame on the object as the task frame.

4 Controller

Impedance control enforces a relationship between force and velocity and has been shown to be a valid concept for a robot that interacts with its environment [21]. In the multiple-manipulator system, the environment each manipulator interacts with consists of the object or objects being manipulated and the other manipulators. Since our objective is to simultaneously control the motion of objects and the internal force and not the total forces of interaction, impedance control for cooperating manipulators should enforce a relationship between the internal force and velocity. If the force in the impedance relationship is the total force imposed by the environment on the manipulator, then object dynamics will contribute to tracking and steady-state position error of the object or objects. One possible impedance that each manipulator may be given is the following linear second-order function

$$M_i \delta \ddot{x}_i + B_i \delta \dot{x}_i + K_i \delta x_i = \delta \tilde{f}_{Ii} \tag{9}$$

where $\delta x_i = x_{id} - x_i =$ Cartesian position and orientation error of the ith robot end effector

$\delta \tilde{f}_{Ii} = \tilde{f}_{Ii} - \tilde{f}_{Iid} =$ internal force error at the ith robot end effector

$M_i,\ B_i,\ K_i =$ desired inertia, damping, and stiffness matrices for the ith robot.

The subscript d denotes a desired quantity.

Each manipulator's end-effector velocity is related to its joint velocity by its Jacobian

$$\dot{x}_i = J_i \dot{q}_i. \tag{10}$$

Differentiating (10) and solving for $\ddot{q}_i$ yields

$$\ddot{q}_i = J_i^{-1}(\ddot{x}_i - \dot{J}_i \dot{q}_i). \tag{11}$$

Solving equation (9) for $\ddot{x}_i$, substituting into equation (11), and incorporating into each manipulators dynamic equation (1), yields the following control law for each robot:

$$\tau_i = D_i\{J_i^{-1}(M_i^{-1}[M_i\ddot{x}_{id} + B_i\delta\dot{x}_i + K_i\delta x_i - \delta\tilde{f}_{Ii}] - \dot{J}_i\dot{q}_i)\} + E_i + J_i^T\tilde{f}_i. \tag{12}$$

Thus, given a desired trajectory, x_{id} and $\tilde{f}_{Iid}$, and measuring position, x_i, and end effector force, $\tilde{f}_i$, the required joint torque can be computed. The actual Cartesian end-effector position for each manipulator can be computed from the measured joint angles of each manipulator and the forward kinematics. The actual internal force, $\tilde{f}_{Ii}$, is computed from equation (5) from the forces, $\tilde{f}$, sensed at all of the end effectors. The internal impedance controller is depicted in Figure 2.

The commanded internal force must be chosen to lie in the range of the internal force projection operator, $I - J_o^{T\#}J_o^T$, which is rank $6n-6$. That is, $\tilde{f}_{Id} = B_I y$ where B_I is a basis for $I - J_o^{T\#}J_o^T$ and y is a $(6n-6)\times 1$ vector representing the commanded internal force. For example, for $n = 2$ a basis for $I - J_o^{T\#}J_o^T$ is

$$B_I = \begin{bmatrix} I_6 \\ -J_{o2}^{-T}J_{o1}^T \end{bmatrix}. \tag{13}$$

Then $\tilde{f}_{I1} = y$ and $\tilde{f}_{I2} = -J_{o2}^{-T}J_{o1}^T\tilde{f}_{I1}$. Thus, we may choose the internal force as seen at end-effector 1 and use (13) to compute the desired internal force as seen at end-effector 2.

Internal force-based impedance control has the following advantages over schemes previously proposed:

1. Internal force-based impedance control is a unified concept in that separate force and position control loops are not required.

2. Internal force is used in the impedance relationship, and, thus, the object dynamics do not contribute to tracking and steady-state position error of the object.

3. Internal force is computed from sensed force via kinematic relationships and, therefore, knowledge of the object dynamics are not required.

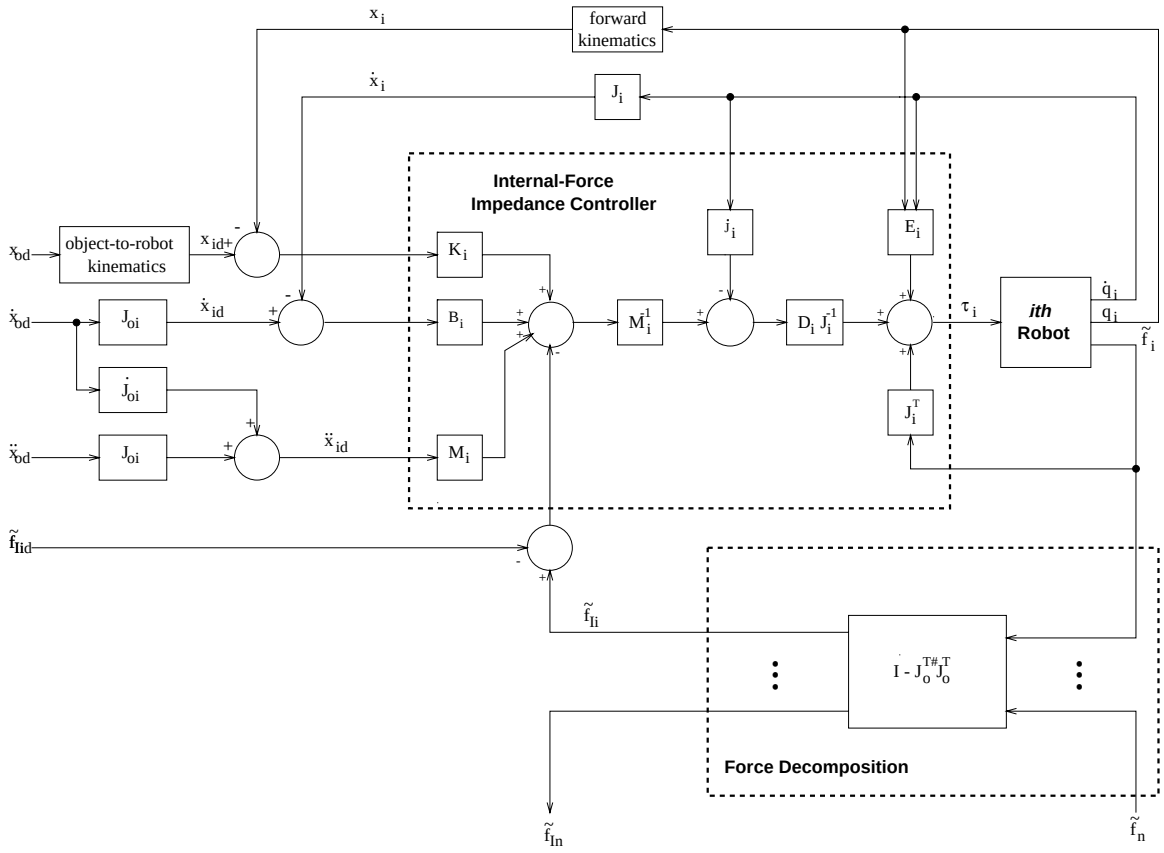

Figure 2: Internal Force-Based Impedance Controller

The same control law (12) is used to control the robots during both constrained and unconstrained operation. It also has the desirable feature of being implemented in Cartesian space and, thus, the inverse kinematics are not required.

5 Stability

The first and foremost requirement for any control algorithm is that the system be stable. Conditions for stability of the multiple-robot system employing control algorithm (12) are stated as the following theorem:

Theorem. If M_i, B_i, and K_i in control law (12) are symmetric positive definite and each robot's Jacobian, J_i, is nonsingular, the system is stable.

Proof. To show stability of the overall system, we first define the error state space vector to be

$$e = [\delta x^T \ \delta \dot{x}^T]^T \tag{14}$$

where $\delta x = [\delta x_1^T \ \delta x_2^T \ldots \delta x_n^T]^T$ for $i = 1$ to n. We also define the following combined impedance matrices $M = diag\{M_i\}$, $B = diag\{B_i\}$, and $K = diag\{K_i\}$.

From Lyapunov theory [22] the system is asymptotically stable if there exists a scalar function V of the state e with continuous first order derivatives such that

1. $V(e)$ is positive definite,
2. $V(e) \to \infty$ as $\|e\| \to \infty$,
3. $\dot{V}(e)$ is negative semi-definite ,

We choose the following Lyapunov function candidate

$$V = \frac{1}{2}\delta \dot{x}^T M \delta \dot{x} + \frac{1}{2}\delta x^T K \delta x. \tag{15}$$

Since all M_i and K_i are symmetric positive definite, so are M and K. Therefore, V is positive definite and condition 1 is satisfied. V also satisfies condition 2.

Taking the derivative of V with respect to time, we get

$$\dot{V} = \delta \dot{x}^T M \delta \ddot{x} + \delta \dot{x}^T K \delta x \tag{16}$$

$$\text{or } \dot{V} = \delta \dot{x}^T (M \delta \ddot{x} + K \delta x). \tag{17}$$

Substituting the control law (12) into the dynamic equation for each robot (1) yields the impedance relationship (9). Solving (9) for $M\delta\ddot{x} + K\delta x$ and substituting into (17) we get

$$\dot{V} = \delta \dot{x}^T \delta \tilde{f}_I - \delta \dot{x}^T B \delta \dot{x}. \tag{18}$$

The end effector velocities are related to the object velocity via the object Jacobian

$$\delta \dot{x} = J_o \delta \dot{x}_o \tag{19}$$

where $\dot{x}_o$ = velocity of the object. Substituting (19) into (17) yields

$$\dot{V} = \delta\dot{x}_o^T J_o^T \delta\tilde{f}_I - \delta\dot{x}^T B \delta\dot{x}. \tag{20}$$

Since $\delta\tilde{f}_I$ lies in the null space of J_o^T, the first term on the right is zero and

$$\dot{V} = -\delta\dot{x}^T B \delta\dot{x} \leq 0. \tag{21}$$

Since each B_i is symmetric positive definite, so is B. Thus, $\dot{V}$ is negative semi-definite and condition 3 is satisfied. Thus, the system is stable. □

To extend the proof to further show that the system is asymptotically stable, we need to show that the system cannot get stuck at some $\delta x \neq 0$. We define G to be largest invariant set in $R = \{e|\dot{V}(e) = 0\}$. By LaSalle's invariant set theorem [22], e asymptotically converges to G as $t \to \infty$. Using the fact that $\delta\dot{x} = 0$ when $\dot{V} = 0$ and (9), we get that the largest invariant set in R is

$$G = \{e \mid \delta\dot{x} = 0,\ K\delta x = \delta\tilde{f}_I\}. \tag{22}$$

Thus, at convergence

$$K\delta x = \delta\tilde{f}_I. \tag{23}$$

Multiplying (23) by J_o^T and using the fact that $\delta\tilde{f}_I$ lies in the null space of J_o^T, we get

$$J_o^T K \delta x = J_o^T \delta\tilde{f}_I = 0 \tag{24}$$

$$\text{or } J_{o1}^T K_1 \delta x_1 + J_{o2}^T K_2 \delta x_2 + \ldots + J_{on}^T K_n \delta x_n = 0. \tag{25}$$

Since the manipulators grasp the object rigidly, kinematic constraints exist among the manipulators. For ease of analysis we will examine the two-arm case, but the results may be extended to any number of arms in a similar fashion. The following kinematic constraints exist between the two manipulators rigidly grasping an object:

$$x_{1t} + R_1 p_{12} = x_{2t} \tag{26}$$

$$R_1^T R_2 = R_{12} \tag{27}$$

where the subscript t denotes Cartesian position component of x, R_i is the rotation matrix for the ith manipulator, p_{12} is a constant vector from the first end-effector frame to the second end-effector frame expressed in the first end-effector frame, and R_{12} is a constant matrix representing the orientation of the second end-effector frame with respect to the first end-effector frame.

In error space the position constraint (26) becomes

$$\delta x_{1t} + \delta R_1 p_{12} = \delta x_{2t} \tag{28}$$

where $\delta x_{it} = x_{itd} - x_{it}$ and $\delta R_1 = R_{1d} - R_1$. The subscript d denotes a desired quantity. The orientation error may be expressed as a rotation matrix as $R_{ei} = R_{id} R_i^T$. From the orientation constraint (27) we get

$$R_1^T R_2 = R_{1d}^T R_{2d} \;\Rightarrow\; R_{1d} R_1^T = R_{2d} R_2^T \;\Rightarrow\; R_{e1} = R_{e2} \;\Rightarrow\; \delta x_{1o} = \delta x_{2o} \tag{29}$$

where the subscript o denotes orientation. Thus, the kinematic constraints require that the orientation errors are equal.

Combining (25), (28), and (29) we get the total set of constraints

$$\begin{bmatrix} J_{o1}^T K_1 & J_{o2}^T K_2 \\ I_6 & -I_6 \end{bmatrix} \delta x + \begin{bmatrix} 0_{6\times 1} \\ \delta R_1 p_{12} \\ 0_{3\times 1} \end{bmatrix} = 0_{12\times 1}. \tag{30}$$

The second term in (30) is a nonlinear function of the desired and actual orientation of the first end-effector frame. If the orientation error is zero, the second term is zero and the position error is zero since it can be shown that the first matrix has full rank and null space equal to $\{0\}$. Thus, $G = \{0\}$ and the system is asymptotically stable. It can also be shown from (28) that if the position error is zero, so is the orientation error and $G = \{0\}$. Note also that if there is no object, $p_{12} = 0_{3x1}$ and $G = \{0\}$. However, the nonlinearity of the second term makes it difficult to prove that the only solution to (30) is $\delta x = 0$ although we conjecture that it is. A rigorous proof is left to future work. Thus, the system has been shown to be stable, but not asymptotically stable.

6 Computational Delays

The control law (12) and the stability proof in section 5 apply to the continuous-time case. In practice the control law will be implemented digitally. Computational delays can affect the stability of the system and place bounds on the values of the parameters chosen in the impedance relationship (9). Since the control law (12) is also intended to be used during the unconstrained phase prior to the robots grasping or squeezing the object to be handled, the effects of digital implementation of the control law on a single manipulator is first analyzed. The effects of computational delays on a dual-manipulator system interacting with a common object is then analyzed.

6.1 Single Manipulator

When the internal force-based impedance control law is used by a single manipulator, internal force is not applicable since the manipulator is not interacting with an object and other manipulators. If the manipulator is moving in free space, the environment imposes no force on the end effector. This is referred to as unconstrained operation. It is possible that the manipulator may come in contact with a rigid surface. In this case the total force appearing at the end effector is used for $\tilde{f}_I$ in the control law. This is referred to as constrained operation. Both cases for single-manipulator operation are analyzed in the following sections.

6.1.1 Unconstrained Manipulator

In the analysis that follows, the assumption is made that the sampling time is sufficiently small such that the robot nonlinearities are effectively canceled by the inner loop control law

$$\tau = DJ^{-1}(u - \dot{J}\dot{q}) + E. \tag{31}$$

Substituting (31) into (1) results in the decoupled double integrator system

$$\ddot{x} = u. \tag{32}$$

Define the state to be

$$X = \begin{bmatrix} x \\ \dot{x} \end{bmatrix}. \tag{33}$$

where x is a vector of Cartesian position and orientation of the end effector. With a zero-order-hold (ZOH) on the input, (32) becomes along each degree of freedom

$$X_{k+1} = \begin{bmatrix} 1 & T_s \\ 0 & 1 \end{bmatrix} X_k + \begin{bmatrix} T_s^2/2 \\ T_s \end{bmatrix} u_k = \Phi X_k + , \, u_k. \tag{34}$$

where T_s = the sampling period and k.

We restrict the analysis to the case where M, B, and K are diagonal so that the system remains decoupled along each degree of freedom. We will denote the inertia, damping, and stiffness along the jth degree of freedom by m_j, b_j, and k_j, respectively. The impedance controller (9) along the jth degree of freedom is described by

$$u_{jk} = -\frac{k_j}{m_j} x_{jk} - \frac{b_j}{m_j} \dot{x}_{jk} + \ddot{x}_{djk} + \frac{b_j}{m_j} \dot{x}_{djk} + \frac{k_j}{m_j} x_{djk} \tag{35}$$

$$\text{or } u_{jk} = -K_{cj} X_{jk} + N_j r_{jk}. \tag{36}$$

where $K_{cj} = [\frac{k_j}{m_j} \quad \frac{b_j}{m_j}]$, $N_j = [\frac{k_j}{m_j} \quad \frac{b_j}{m_j} \quad 1]$, and $r_{jk} = [x_{djk} \quad \dot{x}_{djk} \quad \ddot{x}_{djk}]^T$ = the reference input for jth degree of freedom. Substituting (36) into (34), we get the closed-loop state equation along the jth of freedom

$$X_{j(k+1)} = [\Phi - , \, K_{cj}] X_{jk} + , \, N_j r_{jk} = \Phi_{cj} X_{jk} + , \, N_j r_{jk} \tag{37}$$

$$\Phi_{cj} = \begin{bmatrix} 1 - \frac{T_s^2 k_j}{2m_j} & T_s - \frac{T_s^2 b_j}{2m_j} \\ -\frac{T_s k_j}{m_j} & 1 - \frac{T_s b_j}{m_j} \end{bmatrix}. \tag{38}$$

The stability of the discrete-time system (37) is determined by the eigenvalues of Φ_{cj}. The system will be exponentially stable if the magnitudes of the eigenvalues of Φ_{cj} are all

less than one. Using the Jury test on Φ_{cj} we get the following inequality which expresses the bounds on the impedance parameters:

$$\frac{T_s k_j}{2} < b_j < \frac{2m_j}{T_s}. \tag{39}$$

Thus, for a given sampling period m_j, b_j, and k_j must be chosen to satisfy (39). It is important to note that it is possible to chose m_j and k_j such that no b_j can be found which will result in system stability. K primarily controls the positional accuracy of the robot while M determines the bandwidth. There is a tradeoff between the two. There is a limit as to how much the desired endpoint inertia, M, of the robot can be reduced. The limit on M is even more severe in the constrained case due to the effect of force feedback as we shall see in the next section.

6.1.2 Constrained Manipulator

The constrained case is defined as the manipulator motion being completely restricted. The analysis may be applied to the case of the manipulator in contact with a rigid surface. Once the manipulator breaks contact, then the analysis of the previous section applies. While in contact with a completely rigid surface, the analysis of this section is applicable.

The problem of contact stability has been examined in [23, 24, 25, 26, 27]. In [23, 24] instability is attributed to noncolocation of the sensor and actuators. In [25] impedance control is implemented by feeding back the force error through a compliance function and transforming it to a trajectory correction. To assure stability the gain of the compliance function is limited by the gain of the position controller. The analysis is not applicable to internal force-based impedance control as the structure of the controller proposed in this paper is different.

The effect of delays in impedance control is analyzed in [26], but the analysis is carried out in the continuous-time domain and is not applicable to digital implementations. Also, only stiffness and damping terms are considered. Digital implementations of stiffness and

damping control were examined in [27] which showed a tradeoff between bandwidth and the stiffness of the environment. In the following analysis, we show that there is a limitation on the size of the controller inertia matrix when internal force-based impedance control is implemented digitally.

Substituting the control law (12) with $\delta\tilde{f}$ replacing $\delta\tilde{f}_I$ into the dynamic equation for the manipulator (1), yields in the continuous-time case

$$J^T\tilde{f} = -DJ^{-1}M^{-1}\delta\tilde{f} + J^T\tilde{f} \tag{40}$$

where we have used the fact that in the constrained case the manipulator is not moving ($\dot{q} = 0$). For the digital case, it is observed that when the left side of (40) is at sample instant $k+1$, the right side (the control input) is at sample instant k due to the one sample delay inherent in the digital controller. The result is the following discrete-time equation

$$\tilde{f}_{k+1} = (I - J^{-T}DJ^{-1}M^{-1})\tilde{f}_k + J^{-T}DJ^{-1}M^{-1}\tilde{f}_{dk} \tag{41}$$

$$\tilde{f}_{k+1} = \Phi_{cl}\tilde{f}_k + , \tilde{f}_{dk}. \tag{42}$$

The stability of the discrete-time system (42) is determined by the eigenvalues of Φ_{cl}. The system will be exponentially stable if the magnitudes of the eigenvalues of Φ_{cl} are all less than one. The term $J^{-T}DJ^{-1}$ is the actual inertia of the manipulator as seen at the end effector. Equation (42) places a bound on how much smaller the desired inertia, M, can be relative to the actual end point inertia of the manipulator. This bound is independent of the sample time. In the scalar case, M cannot be any smaller than one half the mass of the manipulator.

Equation (42) provides conditions for stability under the assumption that the manipulator Jacobian and inertia matrix are known exactly. If this is not true, then equation (42) becomes

$$\tilde{f}_{k+1} = (J^{-T}\hat{J}^T - J^{-T}\hat{D}\hat{J}^{-1}M^{-1})\tilde{f}_k + J^{-T}\hat{D}\hat{J}^{-1}M^{-1}(K\delta x_k + \tilde{f}_{dk}) \tag{43}$$

$$\tilde{f}_{k+1} = \Phi_{cl}\tilde{f}_k + , (K\delta x_k + \tilde{f}_{dk}) \tag{44}$$

where the $\hat{}$ designates as estimated value. An inaccurate estimate of the manipulator Jacobian will affect the boundary, but since it is usually known reasonably well the bound determined by equation (42) will be close to the exact value.

6.2 Multiple-Manipulator System

The problem of analyzing the effects of computational delays on a system of multiple manipulators is more complicated than the single manipulator case. Each manipulator interacts with the object and the other manipulators and its motion is constrained by kinematic relationships among the manipulators and the object. To determine the effect of computational delays we will assume that the manipulators and the object are completely constrained. This is analogous to having the held object in contact with a rigid surface. Although not the most general case, it does yield insight into the control of internal forces in the system. Without this assumption the problem is less mathematically tractable. While the analysis is not directly applicable to the unconstrained case, the results are shown to be conservative in our simulations studies and should yield sufficient conditions for stability for the unconstrained system. We examine a two-arm system rigidly grasping a rigid object, but the analysis can be extended to a system of n manipulators in a similar fashion.

Substituting the control law (12) into the dynamic equation for each manipulator (1), yields in the continuous-time case

$$J_i^T \tilde{f}_i = -D_i J_i^{-1} M_i^{-1} \delta \tilde{f}_{Ii} + J_i^T \tilde{f}_i \tag{45}$$

where we have used the fact that in the constrained case the manipulator is not moving ($\dot{q} = 0$). For the digital case, it is observed that when the left side of (45) is at sample instant $k+1$, the right side (the control input) is at sample instant k due to the one sample delay inherent in the digital controller. The result is the following discrete-time equation for each manipulator:

$$\tilde{f}_{i(k+1)} = \tilde{f}_{ik} - J_i^{-T} D_i J_i^{-1} M_i^{-1} \tilde{f}_{Iik} + J_i^{-T} D_i J_i^{-1} M_i^{-1} \tilde{f}_{Iidk}. \tag{46}$$

The definition of internal force from (5) is

$$\tilde{f}_{I1k} = \frac{1}{2}(\tilde{f}_{1k} - J_{o1}^{-T} J_{o2}^{T} \tilde{f}_{2k}) \tag{47}$$

$$\tilde{f}_{I2k} = \frac{1}{2}(\tilde{f}_{2k} - J_{o2}^{-T} J_{o1}^{T} \tilde{f}_{1k}). \tag{48}$$

Substituting (47) and (48) into (46) yields

$$\begin{bmatrix} \tilde{f}_{1(k+1)} \\ \tilde{f}_{2(k+1)} \end{bmatrix} = \begin{bmatrix} I - \frac{1}{2} J_1^{-T} D_1 J_1^{-1} M_1^{-1} & \frac{1}{2} J_1^{-T} D_1 J_1^{-1} M_1^{-1} J_{o1}^{-T} J_{o2}^{T} \\ \frac{1}{2} J_2^{-T} D_2 J_2^{-1} M_2^{-1} J_{o2}^{-T} J_{o1}^{T} & I - \frac{1}{2} J_2^{-T} D_2 J_2^{-1} M_2^{-1} \end{bmatrix} \begin{bmatrix} \tilde{f}_{1k} \\ \tilde{f}_{2k} \end{bmatrix} + \begin{bmatrix} J_1^{-T} D_1 J_1^{-1} M_1^{-1} \\ -J_2^{-T} D_2 J_2^{-1} M_2^{-1} J_{o2}^{-T} J_{o1}^{T} \end{bmatrix} \tilde{f}_{I1dk} \tag{49}$$

$$\tilde{f}_{k+1} = A\tilde{f}_k + B\tilde{f}_{I1dk}. \tag{50}$$

The first question we would like to ask about the system (A, B) is whether or not it is reachable. We partition B into

$$B = \begin{bmatrix} B_1 \\ B_2 \end{bmatrix} = \begin{bmatrix} J_1^{-T} D_1 J_1^{-1} M_1^{-1} \\ -J_2^{-T} D_2 J_2^{-1} M_2^{-1} J_{o2}^{-T} J_{o1}^{T} \end{bmatrix}. \tag{51}$$

We can then express A as

$$A = I - \begin{bmatrix} \frac{1}{2} B_1 & -\frac{1}{2} B_1 J_{o1}^{-T} J_{o2}^{T} \\ \frac{1}{2} B_2 & -\frac{1}{2} B_2 J_{o1}^{-T} J_{o2}^{T} \end{bmatrix}. \tag{52}$$

Using the PBH test with $\lambda = 1$, we get

$$\text{rank}[\lambda I - A : B] = \text{rank}\left[I - I + \begin{bmatrix} \frac{1}{2} B_1 & -\frac{1}{2} B_1 J_{o1}^{-T} J_{o2}^{T} \\ \frac{1}{2} B_2 & -\frac{1}{2} B_2 J_{o1}^{-T} J_{o2}^{T} \end{bmatrix} : B \right] \tag{53}$$

$$= \text{rank}[B : B] \tag{54}$$

$$= \text{rank}(B). \tag{55}$$

Since $[\lambda I - A : B]$ is less than full rank, the system (A, B) is not completely reachable.

We use the following transformation to decompose the system into its reachable and unreachable parts

$$T = \begin{bmatrix} 2(I - J_{o1}^{-T} J_{o2}^{T} \Delta^{-1} B^{-1}) J_{o1}^{-T} & J_{o1}^{-T} J_{o2}^{T} \Delta^{-1} \\ -2\Delta^{-1} B_1^{-1} J_{o1}^{-T} & \Delta^{-1} \end{bmatrix} \tag{56}$$

where $\Delta = B_1^{-1} J_{o1}^{-T} J_{o2}^{T} - B_2^{-1}$. The transformed system matrices and state vector are

$$\hat{A} = T^{-1} A T = \begin{bmatrix} I - \frac{1}{2} J_{o1}^{T} B_1 J_{o1}^{-T} + \frac{1}{2} J_{o2}^{T} B_2 J_{o1}^{-T} & 0 \\ 0 & I \end{bmatrix} \tag{57}$$

$$\hat{B} = T^{-1} B = \begin{bmatrix} \frac{1}{2} J_{o1}^{T} B_1 - \frac{1}{2} J_{o2}^{T} B_2 \\ 0 \end{bmatrix} \tag{58}$$

$$\hat{f}_k = T^{-1} \tilde{f}_k = \begin{bmatrix} J_{o1}^{T} \tilde{f}_{I1k} \\ B_1^{-1} \tilde{f}_{1k} - B_2^{-1} \tilde{f}_{2k} \end{bmatrix} \tag{59}$$

$J_{o1}^{T} \tilde{f}_{I1k}$ is the internal force exerted by manipulator 1 at the origin of the object frame. The internal force at the object frame is the reachable part and is characterized by

$$\begin{aligned} \hat{f}_{1(k+1)} &= [I - \frac{1}{2} J_{o1}^{T} J_1^{-T} D_1 J_1^{-1} M_1^{-1} J_{o1}^{-T} - \frac{1}{2} J_{o2}^{T} J_2^{-T} D_2 J_2^{-1} M_2^{-1} J_{o2}^{-T}] \hat{f}_{1k} \\ &+ [\frac{1}{2} J_{o1}^{T} J_1^{-T} D_1 J_1^{-1} M_1^{-1} + \frac{1}{2} J_{o2}^{T} J_2^{-T} D_2 J_2^{-1} M_2^{-1} J_{o2}^{-T} J_{o1}^{T}] \tilde{f}_{I1dk} \end{aligned} \tag{60}$$

$$\hat{f}_{1(k+1)} = \hat{A}_{11} \hat{f}_{1k} + \hat{B}_1 \tilde{f}_{I1dk}. \tag{61}$$

The unreachable part is

$$\hat{f}_{2(k+1)} = \hat{f}_{2k}. \tag{62}$$

The stability of the reachable part is governed by the eigenvalues of $\hat{A}_{11}$. If its eigenvalues are less than one in magnitude, the reachable part is asymptotically stable. The unreachable part has all its eigenvalues equal to one and, therefore, is marginally stable. The system $(\hat{A}, \hat{B})$ (or (A, B)) is BIBO stable if M_1 and M_2 are chosen such that the eigenvalues of the reachable part are less than one in magnitude.

The analysis above has indicated that there is an unreachable part to the totally constrained dual-manipulator system using the proposed control law. What is the significance

of this unreachable part and what is its physical interpretation? The unreachable part as expressed at the object frame is

$$J_{o1}^T \hat{f}_{2k} = J_{o1}^T M_1 J_1 D_1^{-1} J_1^T \tilde{f}_{1k} + J_{o2}^T M_2 J_2 D_2^{-1} J_2^T \tilde{f}_{2k}. \tag{63}$$

where $J_i D_i^{-1} J_i^T$ is the inverse of the ith manipulator end point inertia. Equation (63) represents the sum of the forces exerted by both manipulators as if each had inertia, M_i, expressed at the object frame. The unreachable part of the system $(\hat{A}, \hat{B})$ is an expression of the principle that we cannot simultaneously control both the position of and the net force on the object. In control law (12) we control the position of the object and the internal force which is the reachable part. If we define the output, y_k, to be the internal force as expressed at the object frame, then

$$y_k = \frac{1}{2}[J_{o1}^T \quad -J_{o2}^T]\tilde{f}_k = C\tilde{f}_k = \hat{C}\hat{f}_k \tag{64}$$

where $\hat{C} = CT = [I \;\; 0]$. Since the second element of $\hat{C}$ is zero, the unreachable part has no effect on the output.

6.3 Relationship Between the Single and Dual-Manipulator Systems

We have established a bound on the size of M for both the single and dual-manipulator cases. Since the manipulators may be required to operate independently or cooperatively, we would like to know the relationship between the bounds on M in these two cases. The single-manipulator bound is determined by Φ_{cl} of equation (42), while the dual-manipulator bound is determined by $\hat{A}_{11}$ of equation (61).

To show the relationship between the single and dual-manipulator cases, we first reformulate the bounds based on basic stability definitions. For the constrained single manipulator, an equilibrium point is asymptotically stable if

1. $\forall \epsilon > 0 \; \exists \; \delta(\epsilon) > 0$ such that if $\|\tilde{f}_0\| < \delta$, then $\|\tilde{f}_k\| < \epsilon \; \forall k > 0$;

2. If $\|\tilde{f}_0\| < \delta$, then $\lim_{k\to\infty} \|\tilde{f}_k\| = 0$, where $\tilde{f}_0$ is the initial condition.

To show condition 1, we take the norm of both sides of equation (42) with $\tilde{f}_{dk} = 0$ and using the Cauchy-Schwartz inequality:

$$\|\tilde{f}_{k+1}\| = \|\Phi_{cl}\tilde{f}_k\| \leq \|\Phi_{cl}\|\|\tilde{f}_k\|. \tag{65}$$

If $\|\Phi_{cl}\| < 1$, then $\|\tilde{f}_{k+1}\| < \|\tilde{f}_k\|$. We choose $\delta = \epsilon,$. Then if $\|\Phi_{cl}\| < 1$,

$$\|\tilde{f}_0\| < \delta \Rightarrow \|\tilde{f}_k\| < \delta \Rightarrow \|\tilde{f}_k\| < \epsilon \ \ \forall k > 0. \tag{66}$$

Condition 1 is satisfied if M is chosen such that $\|\Phi_{cl}\| < 1$.

Compliance with condition 2 if $\|\Phi_{cl}\| < 1$ is shown as follows:

$$\lim_{k\to\infty} \|\tilde{f}_{k+1}\| = \lim_{k\to\infty} \|\Phi_{cl}\tilde{f}_k\| \tag{67}$$

$$\lim_{k\to\infty} \|\tilde{f}_{k+1}\| = \lim_{k\to\infty} \|\Phi_{cl}^k\tilde{f}_0\| \tag{68}$$

$$\lim_{k\to\infty} \|\tilde{f}_{k+1}\| \leq \lim_{k\to\infty} \|\Phi_{cl}^k\|\|\tilde{f}_0\| \tag{69}$$

$$\lim_{k\to\infty} \|\tilde{f}_{k+1}\| \leq \lim_{k\to\infty} \rho^k\|\tilde{f}_0\| \ \text{ (where } 0 \leq \rho < 1) \tag{70}$$

$$\lim_{k\to\infty} \|\tilde{f}_{k+1}\| = 0. \tag{71}$$

Thus, the constrained single-manipulator system is asymptotically stable with the proper choice of M.

Now let us examine the reachable part of the constrained dual-manipulator system. First, we note that

$$\hat{A}_{11} = \frac{1}{2}(\Phi_{cl1} + \Phi_{cl2}) \tag{72}$$

$$\|\hat{A}_{11}\| = \|\frac{1}{2}(\Phi_{cl1} + \Phi_{cl2})\| \tag{73}$$

$$\|\hat{A}_{11}\| \leq \frac{1}{2}(\|\Phi_{cl1}\| + \|\Phi_{cl2}\|) \tag{74}$$

where $\Phi_{cli} = I - J_{oi}^T J_i^{-T} D_i J_i^{-1} M_i^{-1} J_{oi}^{-T}$. To show condition 1, we take the norm of both sides of equation (61) with $\tilde{f}_{I1dk} = 0$ and using the Cauchy-Schwartz inequality:

$$\|J_{o1}^T\tilde{f}_{I1(k+1)}\| = \|\hat{A}_{11}J_{o1}^T\tilde{f}_{I1k}\| \leq \|\hat{A}_{11}\|\|J_{o1}^T\tilde{f}_{I1k}\|. \tag{75}$$

If $\|\hat{A}_{11}\| < 1$, then $\|J_{o1}^T \tilde{f}_{I(k+1)}\| < \|J_{o1}^T \tilde{f}_{Ik}\|$. We choose $\delta = \epsilon$,. Then if $\|\hat{A}_{11}\| < 1$,

$$\|J_{o1}^T \tilde{f}_{I10}\| < \delta \Rightarrow \|J_{o1}^T \tilde{f}_{I1k}\| < \delta \Rightarrow \|J_{o1}^T \tilde{f}_{I1k}\| < \epsilon \ \ \forall k > 0. \tag{76}$$

Condition 1 is satisfied if M_1 and M_2 are chosen such that $\|\hat{A}_{11}\| < 1$. If M_1 and M_2 are chosen such that $\|\Phi_{cl1}\| < 1$ and $\|\Phi_{cl2}\| < 1$, then by (74) $\|\hat{A}_{11}\| < 1$ and condition 1 is satisfied.

Compliance with condition 2 can be shown as in the single-manipulator case if $\|\hat{A}_{11}\| < 1$. Thus, if the M of each manipulator is chosen such that it is asymptotically stable, then the reachable part of the dual-manipulator system is also asymptotically stable. Therefore, with the proper choice of M_1 and M_2 the dual-manipulator system is BIBO stable. It should be pointed out that if M_1 and M_2 are chosen such that each manipulator is individually stable, then this is a conservative choice for the dual-manipulator case. There are choices of M_1 and M_2 such that the individual manipulators would be unstable, but the constrained dual-manipulator system is stable.

7 Simulation

7.1 System Dynamic Equations

In order to simulate a multiple-manipulator system using the proposed control law, a dynamic equation for the complete system is required. The system consists of n six-link manipulators handling an object. We first define the following system matrices:

$$\tau = \begin{bmatrix} \tau_1 \\ \vdots \\ \tau_n \end{bmatrix}, \ q = \begin{bmatrix} q_1 \\ \vdots \\ q_n \end{bmatrix}, \ D = \begin{bmatrix} D_1 & & 0 \\ & \ddots & \\ 0 & & D_n \end{bmatrix}, \ E = \begin{bmatrix} E_1 \\ \vdots \\ E_n \end{bmatrix}, \ J = \begin{bmatrix} J_1 & & 0 \\ & \ddots & \\ 0 & & J_n \end{bmatrix}$$

where the subscript denotes which manipulator.

The dynamic equation for each manipulator was given in equation (1). The dynamic

equation for the object is

$$J_o^T \tilde{f} = D_o(x_o)\ddot{x}_o + E_o(\dot{x}_o, x_o) \tag{77}$$

where $D_o(x_o)$ is the inertia matrix of the object, $E_o(x_o, \dot{x}_o)$ is the Coriolis and gravity vector, and x_o is the Cartesian position of the object. Combining all the dynamic equations, we get

$$\begin{bmatrix} J_o^T \\ J^T \end{bmatrix} \tilde{f} = \begin{bmatrix} D_o\ddot{x}_o + E_o \\ \tau - D\ddot{q} - E \end{bmatrix}. \tag{78}$$

Equation (78) represents a system of $6 + 6n$ simultaneous equations with $6 + 12n$ unknowns — six elements of the object acceleration vector, $6n$ joint accelerations, and $6n$ forces. Thus, (78) is an under-determined system. In [28] constraint equations on the velocity for the rigid-grasp case were used to eliminate $\tilde{f}$ and $\ddot{x}_o$ from equation (78) for a two-arm system. In the following derivation, a systematic method is developed which applies a system of n robots.

The following constraint equation among the velocities of the manipulators and the object:

$$J_o\dot{x}_o = J\dot{q}. \tag{79}$$

Solving (79) for the object velocity, we get

$$\dot{x}_o = J_o^+ J\dot{q}. \tag{80}$$

Equation (80) is an exact solution as J_o is $6n \times 6$ and has full-column rank. The object velocity along with the object position, which can be determined by the kinematics, are used to compute $E_o(\dot{x}_o, x_o)$. Differentiating (79) and solving for $\ddot{x}_o$ in terms of joint variables, we get

$$\ddot{x}_o = J_o^+ J\ddot{q} + J_o^+(\dot{J} - \dot{J}_o J_o^+ J)\dot{q}. \tag{81}$$

Equation (81) is used to eliminate the object acceleration, $\ddot{x}_o$, from equation (78).

To get the necessary equations which may be added to (78) to form a completely determined system, we substitute (80) into (79) to get

$$(J - J_o J_o^+ J)\dot{q} \;\; = \;\; 0 \tag{82}$$

$$J_4\dot{q} \;=\; 0. \tag{83}$$

Differentiating (83), we get

$$J_4\ddot{q} + \dot{J}_4\dot{q} = 0 \tag{84}$$

where $\dot{J}_4 = \dot{J} - \dot{J}_o J_o^+ J - J_o \dot{J}_o^+ J - J_o J_0^+ \dot{J}$. We only need $6n-6$ independent rows of (84). Defining $\tilde{J}_4$ as $6n-6$ independent rows of J_4, we get

$$\tilde{J}_4\ddot{q} + \dot{\tilde{J}}_4\dot{q} = 0. \tag{85}$$

Combining equations (78), (81), and (85), we get

$$\begin{bmatrix} J_o^T \\ J^T \\ 0_{6n-6\times 6n} \end{bmatrix} \tilde{f} \;=\; \begin{bmatrix} D_o J_o^+ J \\ -D \\ \tilde{J}_4 \end{bmatrix} \ddot{q} + \begin{bmatrix} D_o J_o^+ (\dot{J} - \dot{J}_o J_o^+ J)\dot{q} + E_o \\ \tau - E \\ \dot{\tilde{J}}_4\dot{q} \end{bmatrix} \tag{86}$$

$$J_3\tilde{f} \;=\; D_3\ddot{q} + E_3 \tag{87}$$

Equation (87) represents a system of $12n$ equations in $12n$ unknowns and can be solved exactly for the forces in terms of the joint accelerations since J_3 is full-column rank to get

$$\tilde{f} = J_3^+(D_3\ddot{q} + E_3). \tag{88}$$

Substituting (88) into (87) and solving for the joint acceleration, we get

$$\ddot{q} = (J_3 J_3^+ D_3 - D_3)^+ (I_{12n} - J_3 J_3^+)E_3. \tag{89}$$

The right side of equation (89) is only a function of the joint positions, joint velocities, and input torques. Thus, it may be used by the simulator to compute the joint accelerations at each integration step. The above procedure applies to a system in which the manipulators rigidly grasp the object, but can be applied in a similar manner to a system with non-rigid or mixed grasps.

Table 1: Manipulator and Object Parameters

item	value
link 1 length/mass	1m/1Kg
link 2 length/mass	1m/1Kg
link 3 length/mass	0.5m/0.5Kg
object radius/mass	0.5m/0.2Kg

7.2 Simulation Results

The internal force-based impedance controller was simulated on a system consisting of two 3-link planar manipulators rigidly holding a spherical object as depicted in Figure 3. The dynamic model for each manipulator was taken from [29]. The link and object parameters are given in Table 1. The object inertia matrix and Coriolis and gravity vector are

$$D_o = \begin{bmatrix} 0.2 & 0 & 0 \\ 0 & 0.2 & 0 \\ 0 & 0 & 0.02 \end{bmatrix}, \quad E_o = \begin{bmatrix} 0 \\ 1.96 \\ 0 \end{bmatrix}. \tag{90}$$

The motion of the manipulators and the object is depicted in Figure 3. The desired object trajectory is based on a quintic polynomial and consists of moving the object 0.5m in the x direction, -0.5m in the y direction, and a rotation of 45 degrees in 0.5 seconds with the desired internal force, $\tilde{f}_{Id}$, equal to zero. The commanded trajectory of the object is shown in Figure 4.

Each manipulator impedance was chosen using the conditions derived in section 6 by examining the actual end point inertia of each manipulator throughout the desired trajectory. The inertia matrix, M, of each manipulator impedance was chosen to be small within the stability bound of (61). Making M too small results in instability even when simulating a continuous-time system because the bound on M is independent of the sample period which

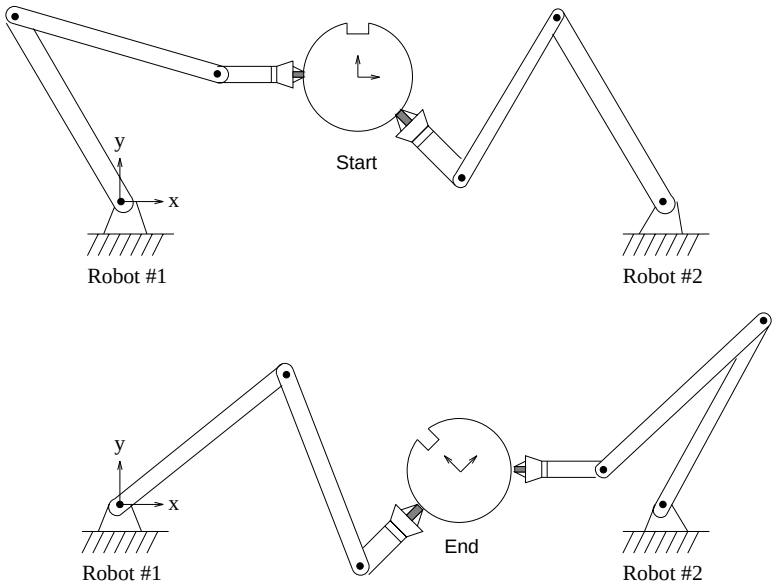

Figure 3: Planar Dual-Manipulator System

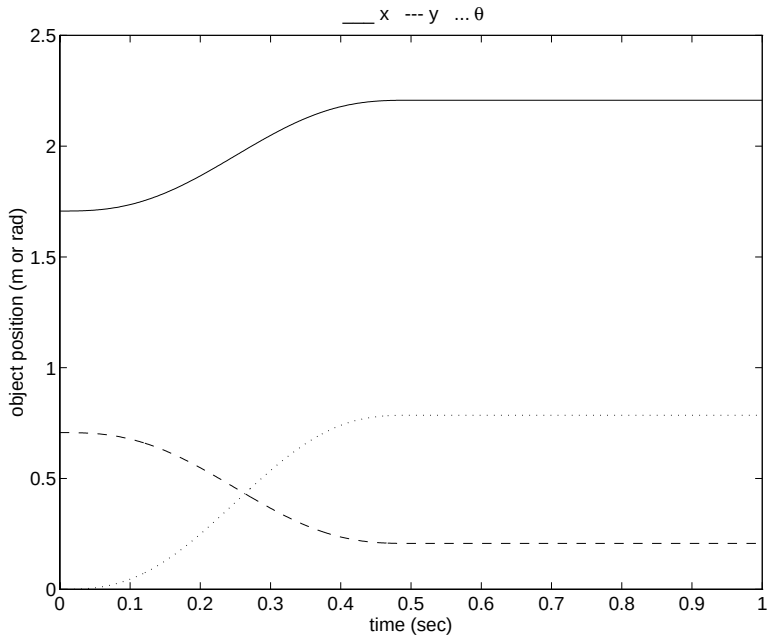

Figure 4: Commanded Object Trajectory

in a continuous-time simulation is the integration time step. The stiffness matrix, K, for each manipulator was chosen such that an impedance bandwidth of approximately 3 Hz is achieved along each degree of freedom, and B was chosen to achieve critical damping. The inertia, damping, and stiffness matrices of each impedance relationship were

$$M_i = \begin{bmatrix} 3 & 0 & 0 \\ 0 & 3 & 0 \\ 0 & 0 & 1 \end{bmatrix}, \; B_i = \begin{bmatrix} 190 & 0 & 0 \\ 0 & 190 & 0 \\ 0 & 0 & 63 \end{bmatrix}, \; K_i = \begin{bmatrix} 3000 & 0 & 0 \\ 0 & 3000 & 0 \\ 0 & 0 & 1000 \end{bmatrix}. \quad (91)$$

The errors of the object position and internal force from the desired trajectory are shown in Figure 5. The position errors are under 0.03mm and 0.01mrad during the motion and go to zero in the steady state. The internal force is controlled within 0.1N and 0.14Nm of the desired and goes to zero in the steady state.

To see the effect of the inertia on the internal force, M was increased to M=*diag*{6,6,2} with $K = 1000M$ to keep the bandwidth at 3Hz and B chosen to achieve critical damping. Figure 6 shows the position tracking error and the internal force. As expected, the larger value of impedance inertia causes higher internal force (0.23N and 0.28Nm max) during the object motion. This suggest reducing M to minimize internal force error. Of course, there is a limit to how much the actual manipulator inertia can be reduced without violating the stability conditions. The effect of increasing M on position error (0.043mm and 0.013mrad max) during the motion is less pronounced.

An interesting choice of impedance inertia is to set it equal to the actual end point inertia of the manipulator. That is, $M_i = J_i^{-T} D_i J_i^{-1}$. This choice of inertia assures that the stability constraints of section 6 are met. Over the commanded trajectory the largest singular values of M_1 and M_2 vary from 2.1 to 2.5 Kg and 1.5 to 2.6 Kg, respectively. Again, to achieve the 3Hz bandwidth along each degree of freedom, K was chosen to be $1000M$. Figure 7 shows the position error and internal force. Position is controlled to within 0.006mm and 0.002mrad and internal force is controlled to within 0.12N and 0.08Nm.

Finally, the system was simulated with error in the kinematic model of the manipulator.

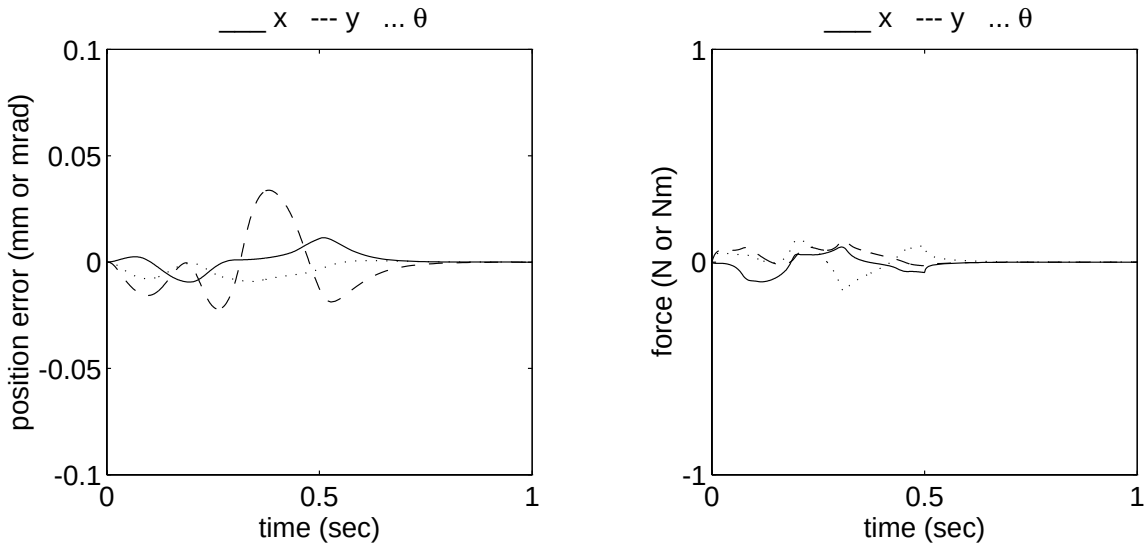

Figure 5: Object Position Error & Internal Force - M=*diag*{3,3,1}, K=1000M

The length of link 1 in the model used by the controller was 1.001m instead of the true value of 1m. The impedance parameters were M=*diag*{3,3,1}, B=*diag*{190,190,63} and K=1000M. Figure 8 shows the internal force as expressed at the object frame for the same motion as before. There is approximately 0.7mm and 0.25mrad of steady-state position error and 0.35N and 0.05Nm of steady-state internal force. This steady-state internal force is directly proportional to the stiffness matrix, K, in the impedance relationship and the amount of kinematic error in the model. At steady-state the governing relationship is $K\delta x_i = \delta f_{Ii}$. Thus, the controller is robust with respect to kinematic errors.

The simulations validate that the internal force-based impedance controller for multiple-manipulator systems is a viable control scheme that can simultaneously control the position of the object being manipulated and the internal force. Careful choice of the inertia, damping, and stiffness matrices in the impedance relationship is important in achieving good system performance. Extensive simulations also indicate that the system is asymptotically stable.

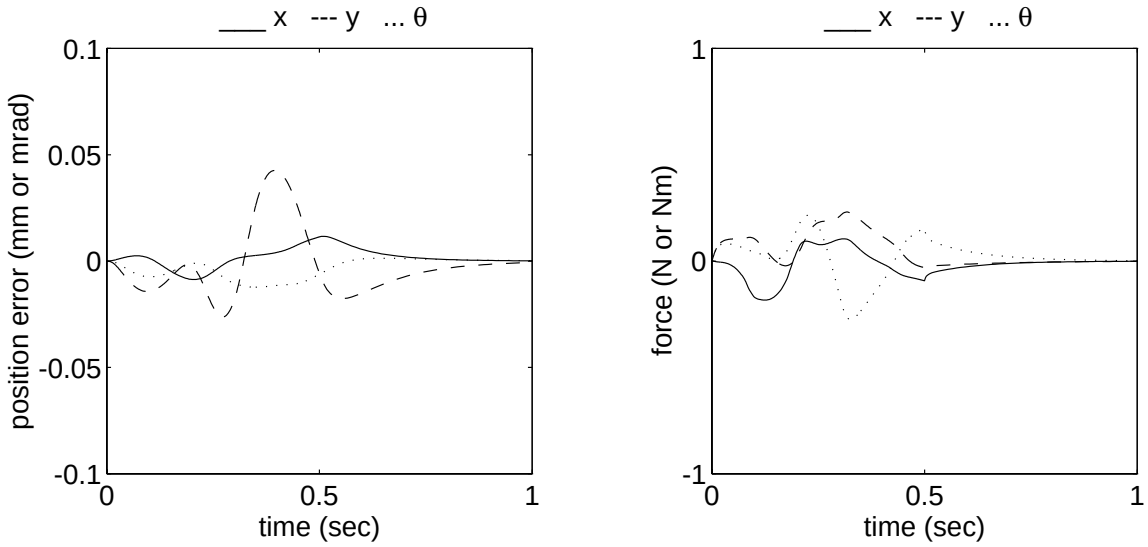

Figure 6: Object Position Error & Internal Force - M=$diag$\{6,6,2\}, K=1000M

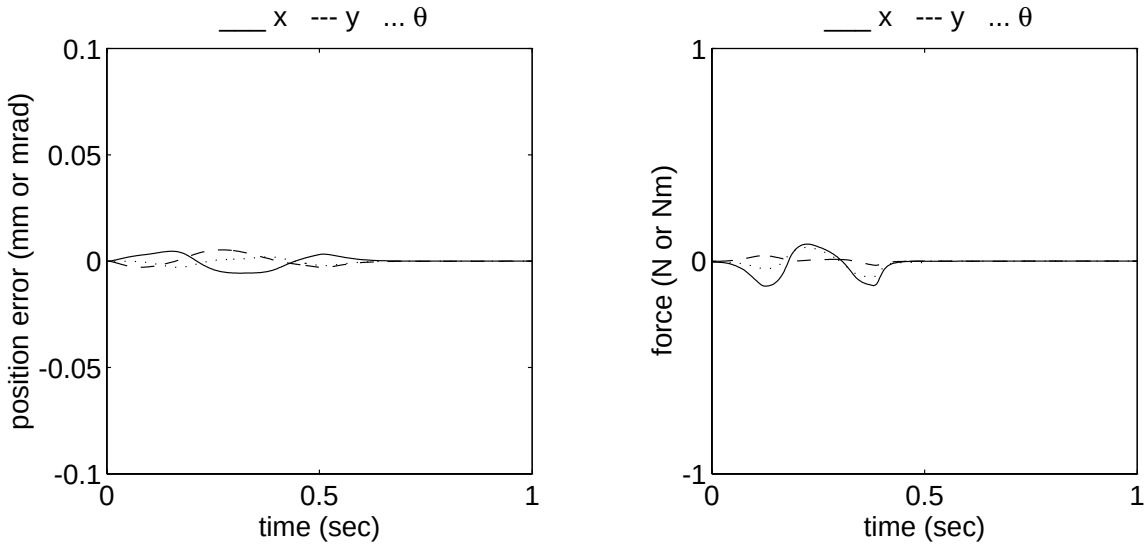

Figure 7: Object Position Error & Internal Force - M=$J^{-T}DJ^{-1}$, K=1000M

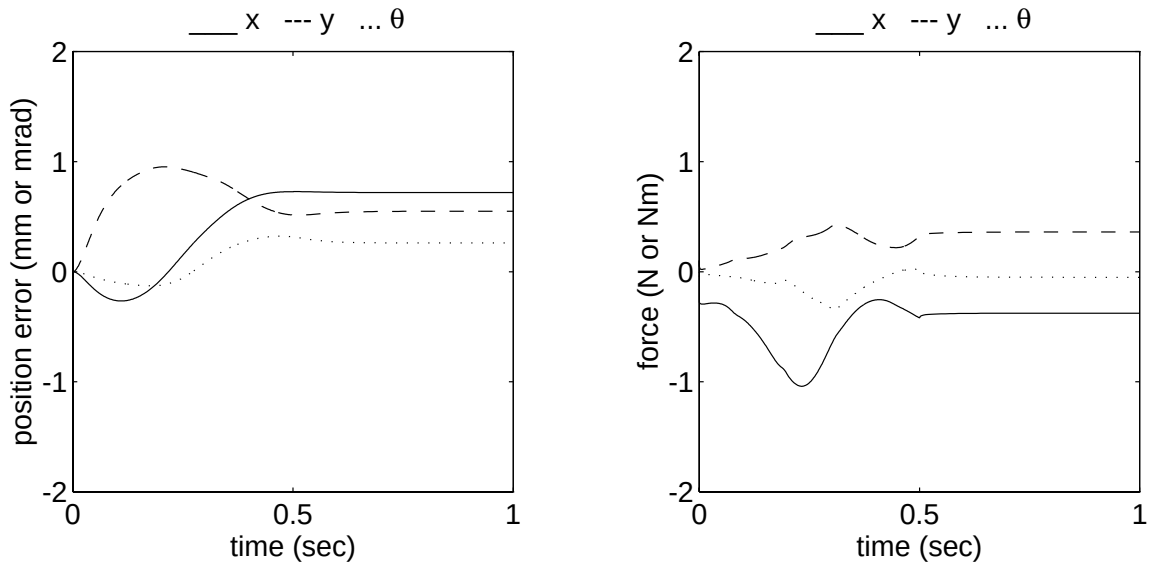

Figure 8: Object Position Error & Internal Force - Kinematic Error in the Model

8 Conclusion

The proposed internal force-based impedance controller for multiple cooperating manipulators enforces a relationship between the velocity of each manipulator and the internal force on the objects being manipulated. It has several desirable features which are advantages over previously proposed schemes. Each manipulator is directly given the property of an impedance by the controller eliminating the gain limitation of previous schemes. Internal force, which is computed from sensed force via kinematic relationships, is used in the impedance relationship which eliminates the need to know the object dynamics and reduces their effect on tracking and steady-state error.

The system was shown to be stable with the proper choice of manipulator impedances. The effects of computational delays were analyzed vis-a-vis stability and a lower bound derived on the size of the desired manipulator inertia relative to the actual manipulator endpoint inertia. The bound is independent of the sample time. Simulations on a two-manipulator system showed the validity of the internal force-base impedance controller in simultaneously controlling the motion of the object along with the internal force.

References

[1] P. Dauchez, X. Delebarre, Y. Bouffard, and E. Degoulange, "Task modeling and force control for a two-arm robot," in *Proceedings of the IEEE International Conference on Robotics and Automation*, pp. 1702–1707, 1991.

[2] S. Hayati, "Hybrid position/force control of multi-arm cooperating robots," in *Proceedings of the IEEE International Conference on Robotics and Automation*, pp. 82–89, 1986.

[3] Y. Hu and A. Goldenberg, "An adaptive approach to motion and force control of multiple coordinated robot arms," in *Proceedings of the IEEE International Conference on Robotics and Automation*, pp. 1091–1096, 1989.

[4] C. Kopf, "Two arm hybrid position/force control with dynamic compensation," in *Robots and Manufacturing*, (New York, NY), pp. 371–380, ASME Press, 1988.

[5] V. Kumar, X. Yun, E. Paljug, and N. Sarkar, "Control of contact conditions for manipulation with multiple robotic systems," in *Proceedings of the IEEE International Conference on Robotics and Automation*, pp. 170–175, Apr. 1991.

[6] M. Uchiyama and P. Dauchez, "A symmetric hybrid position/force control scheme for the coordination of two robots," in *Proceedings of the IEEE International Conference on Robotics and Automation*, pp. 350–356, 1988.

[7] M. Uchiyama, N. Iwasawa, and K. Hakomori, "Hybrid position/force control for coordination of a two-arm robot," in *Proceedings of the IEEE International Conference on Robotics and Automation*, pp. 1242–1247, 1987.

[8] M. Unseren, "A new technique for dynamic load distribution when two manipulators mutually lift a rigid object, part 1: The proposed technique, part 2: Derivation of entire system model and control architecture," in *Proceedings of the World Automation Congress, Intelligent Automation and Soft Computing, Trends in Research, Development, and Applications*, pp. 359–372, TSI Press, 1994.

[9] S. Arimoto, F. Miyazaki, and S. Kawamura, "Cooperative motion control of multiple robot arms or fingers," in *Proceedings of the IEEE International Conference on Robotics and Automation*, pp. 1407–1412, 1987.

[10] S. Hayati, K. Tso, and T. Lee, "Generalized master/slave coordination and control for a dual-arm robotic system," in *Robots and Manufacturing*, (New York, NY), pp. 421–430, ASME Press, 1988.

[11] K. Kosuge, M. Koga, K. Furata, and K. Nosaki, "Coordinated motion control of robot arm based on virtual internal model," in *Proceedings of the IEEE International Conference on Robotics and Automation*, pp. 1097–1102, 1989.

[12] S. Schneider and R. Cannon, "Object impedance control for cooperative manipulation: Theory and experimental results," *IEEE Transactions on Robotics and Automation*, vol. 8, pp. 383–394, June 1992.

[13] J. Tao, J. Luh, and Y. Zheng, "Compliant coordination of two moving robots," *IEEE Transactions on Robotics and Automation*, vol. 6, pp. 322–330, June 1990.

[14] P. Chiacchio, S. Chiaverini, and B. Siciliano, "Cooperative control schemes for multiple robot manipulator systems," in *Proceedings of the IEEE International Conference on Robotics and Automation*, pp. 2218–2223, 1992.

[15] N. Hogan, "Stable execution of contact tasks using impedance control," in *Proceedings of the IEEE International Conference on Robotics and Automation*, pp. 1047–1054, 1987.

[16] H. Kazerooni and T. Tsay, "Compliance control and unstructured modeling of cooperating robots," in *Proceedings of the IEEE International Conference on Robotics and Automation*, pp. 510–515, 1988.

[17] K. Doty, C. Melchiorri, and C. Bonivento, "A theory of generalized inverses applied to robotics," *International Journal of Robotics Research*, vol. 12, pp. 1–19, Feb. 1993.

[18] I. Walker, R. Freeman, and S. Marcus, "Analysis of motion and internal loading of objects grasped by multiple cooperating manipulators," *International Journal of Robotics Research*, vol. 10, pp. 396–409, Aug. 1991.

[19] R. Bonitz and T. Hsia, "Internal force-based impedance control for cooperating manipulators," in *Proceedings of the IEEE International Conference on Robotics and Automation*, vol. 3, pp. 944–949, May 1993.

[20] R. Bonitz and T. Hsia, "Force decomposition in cooperating manipulators using the theory of metric spaces and generalized inverses," in *Proceedings of the IEEE International Conference on Robotics and Automation*, vol. 2, pp. 1521–1527, May 1994.

[21] N. Hogan, "Impedance control: An approach to manipulation: Parts i, ii, iii," *ASME Journal of Dynamic Systems, Measurements, and Control*, vol. 107, pp. 1–24, Mar. 1985.

[22] J. Slotine and W. Li, *Applied Nonlinear Control*. Prentice Hall, 1991.

[23] J. Colgate and N. Hogan, "An analysis of contact instability in terms of passive physical equivalents," in *Proceedings of the IEEE International Conference on Robotics and Automation*, pp. 404–409, 1989.

[24] S. Eppinger and W. Seering, "On dynamic models of robot force control," in *Proceedings of the IEEE International Conference on Robotics and Automation*, pp. 29–34, 1986.

[25] H. Kazerooni, "Robust non-linear impedance control for robot manipulators," in *Proceedings of the IEEE International Conference on Robotics and Automation*, pp. 741–750, 1987.

[26] D. Lawrence, "Impedance control stability properties in common implementations," in *Proceedings of the IEEE International Conference on Robotics and Automation*, pp. 1185–1190, 1988.

[27] D. Whitney, "Historical perspective and state of the art in robot force control," in *Proceedings of the IEEE International Conference on Robotics and Automation*, pp. 262–268, 1985.

[28] M. Unseren and A. Koivo, "Reduced-order model and decoupled-control architecture for two manipulators holding and object," in *Proceedings of the IEEE International Conference on Robotics and Automation*, pp. 1240–1245, 1989.

[29] C. Carignan, "Adaptive tracking for complex systems using reduced-order models," in *Proceedings of the IEEE International Conference on Robotics and Automation*, pp. 2078–2083, 1990.